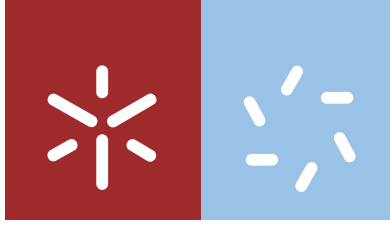Universidade do Minho
Escola de Ciências

Célia de Jesus Sousa Barbosa

Internalization of resveratrol nanoparticles in yeast and bioactivity

Universidade do Minho
Escola de Ciências

Célia de Jesus Sousa Barbosa

Internalization of resveratrol nanoparticles in yeast and bioactivity

Dissertação de Mestrado
Mestrado em Biofísica e Bionanossistemas

Trabalho realizado sob orientação do
Professor Doutor Hernâni Varanda Gerós
e da
Professora Doutora Maria Elisabete Cunha Dias Real Oliveira

março de 2017

DECLARAÇÃO

Nome: Célia de Jesus Sousa Barbosa

Endereço eletrónico: celia.jesus@gmail.com Telefone: 96724689

Número do Bilhete de Identidade: 11941936

Título dissertação: "Internalization of resveratrol nanoparticles in yeast and bioactivity"

Orientador(es): Professor Doutor Hernâni Varanda Gerós e Professora Doutora Maria Elisabete Cunha Dias Real Oliveira

Ano de conclusão: 2017

Designação do Mestrado: Biofísica e Bionanossistemas

Universidade do Minho, ____/____/_____

Assinatura: _____

Acknowledgments:

This dissertation benefited from the insight of several people, directly and indirectly, and for them I express my deepest appreciation. Throughout the course I have had the pleasure to count with the solidarity of my fellow investigators, who have supported and assisted me.

I woud like to thank my advisors, Prof. Hernâni Gerós and Prof. Maria Elisabete Real Oliveira, for their willingness of accepting me into their research groups, granting me all the conditions necessary for the accomplishment of this task, and for sharing with me their knowledge and experience. To Prof. Manuela Côrte-Real, who was always prompt to provide the necessary guidance and encouragement, my deepest thanks.

Also, my eternal gratitude to Dr. Marlene Lucio, Dr. Cátia Pereira and Dr. Viviana Martins, who helped me to take the first steps in the laboratory, and encouraged me in moments of doubt and frustration.

Last but not least, I want to thank my boyfriend and my parents, because if were not for them I would never have dared to venture forth at this stage of my life. For them, who put up with me during this difficult time, because of the stress and despair when my work didn't go well or as expected, a thank you for their words of comfort and comprehension.

Thank you all from the bottom of my heart.

Internalization of resveratrol nanoparticles in yeast and bioactivity

Abstract

Resveratrol (RSV) is a phenolic compound, belonging to a class of chemical compounds derived from phenylalanine with a reactive hydroxyl group (-OH) attached to an aromatic hydrocarbon ring. Several pharmacological effects were attributed to RSV, including antioxidant properties. Different studies have also shown that RSV has a very low bioavailability, which has led to the suspicion that many of the observed health benefits may not be attainable in humans due to its rapid metabolism. To improve bioavailability and pharmacokinetic profile some attempts have been made to encapsulate RSV into a lipid based nanocarrier system, such as liposomes, which are clinically established for drug delivery. The therapeutic efficiency of liposomes systems is highly dependent on the characteristics of lipid molecules, which influence the structure and stability of this type of nanocarriers under physiological conditions. Previous work by our group has shown that liposomes prepared with DODAB:MO (1:2) are promising nanocarriers for delivery of nucleic acids and proteins. Also, these nanocarriers were exploited to load with RSV and important parameters critical for their efficient biological application were assessed. In the scope of the previous research work developed by Inês Ferreira (Master thesis in Biophysics and Bionanosystems, University of Minho, 2015) the DODAB:MO (1:2) liposomal system loaded with RSV revealed adequate characteristics for drug release purposes, high stability and homogeneity, high positive surface charge, and a good as well as a good encapsulation efficiency i.e. the percentage of RSV which is incorporated by liposomal system, (EE%), and the percentage of RSV which is incorporated by total lipid concentration (RL%). In the context of the present study the yeast *Saccharomyces cerevisiae* W303-1A was then used as a cell model to evaluate the biological activity of RSV loaded DODAB:MO (1:2) liposomes. Internalization studies of RSV-loaded liposomes were then performed using fluorescent probes and fluorescence microscopy, and their biological activity was compared with free RSV using ROS-sensitive probes coupled to flow cytometry analysis. After 5 h incubation yeast cells readily internalized liposomes, that appeared as bright blue spots in the periphery of the central vacuole. Moreover, when yeast cells were incubated with DPH alone no fluorescence was detected in the cytosol. When yeast cells were incubated with the lipophilic fluorescent probe FM1-43, results showed that its green fluorescence co-localized with the blue fluorescence of DPH, suggesting that liposomes are efficiently internalized by cells and follow the endocytic pathway. To study the effect of RSV in yeast mitochondrial morphology, the strain *S. cerevisiae W303-1A* Pyx232-mtGFP, which expresses a mitochondrial matrix-targeted GFP was used. Results showed that cells displaying non-fragmented/tubular mitochondrial networks predominate up to 5 h mostly in control conditions, while a the vacuolar/diffuse cytosolic fluorescence predominate after 40 h of incubation either with free or encapsulated RSV. Moreover, the incubation with liposomes containing 200 µM RSV during 45 h was the experimental condition where cells exhibiting the latter phenotype were more abundant.

Internalização e bioatividade do resveratrol em nanopartículas em células de levedura

Resumo

O resveratrol (RSV) é um composto fenólico, pertencente a uma classe de compostos químicos derivados de fenilalanina com um grupo hidroxilo reativo (-OH) ligado a um anel de hidrocarboneto aromático. Vários efeitos farmacológicos têm sido atribuídos a este composto, incluindo propriedades antioxidantes. Vários outros estudos demonstraram que o RSV tem uma biodisponibilidade muito baixa, o que levou a suspeitar que muitos dos potenciais efeitos benéficos para a saúde, poderiam não ser atingíveis em seres humanos devido ao seu rápido metabolismo. Como forma de melhorar a biodisponibilidade e o perfil farmacocinético, foram executadas várias tentativas para encapsular RSV em lipossomas, nanossistemas clinicamente estabelecidos para a administração de fármacos. As eficiências terapêuticas dos lipossomas são dependentes das características das moléculas lipídicas, que influenciam a sua estrutura e a estabilidade em condições fisiológicas. Trabalhos anteriores do nosso grupo mostraram que os lipossomas preparados com o DODAB:MO, são nanossistemas promissores para transporte de ácidos nucleicos e proteínas. No âmbito do trabalho desenvolvido por Inês Ferreira (Tese de Mestrado em Biofísica e Bionanossistemas, Universidade do Minho, 2015), o sistema lipossomal DODAB:MO carregado com RSV, revelou-se com características adequadas para a libertação controlada do RSV, mostrando estabilidade e homogeneidade, carga superficial positiva, bem como uma boa eficiência de encapsulação isto é a percentagem de RSV que é incorporado no sistema lipossomal (EE%) e a percentagem de RSV incorporada relativamente à concentração total de lípido (RL%). No presente estudo, para avaliar a atividade biológica dos nanossistemas foi usada a levedura *Saccharomyces cerevisiae* W303-1A como modelo celular. Para os estudos de internalização dos lipossomas carregados com RSV foram realizados ensaios de microscopia de fluorescência e de citometria de fluxo com sondas fluorescentes apropriadas, e a sua atividade biológica foi comparada com a do RSV livre. Após 5 h de incubação as células de levedura internalizaram eficazmente os lipossomas, que se localizam na periferia do vacúolo central como esferas azuis brilhantes. Quando as células de levedura foram incubadas com a sonda lipofílica fluorescente FM1-43, a fluorescência verde co-localizou com a fluorescência azul do DPH, sugerindo que os lipossomas são internalizados eficientemente pelas células e seguem a via endocítica. Para estudar o efeito do RSV na morfologia mitocondrial de levedura, utilizou-se a estirpe *S. cerevisiae* W303-1A Pyx232-mtGFP a expressar uma GFP na matriz mitocondrial. Nos tempos iniciais de incubação predominaram células com redes mitocondriais não-fragmentadas/tubulares, principalmente nas condições controlo, enquanto quer na presença de RSV livre ou encapsulado durante 40 h, células com fluorescência citosólica/vacuolar difusa eram muito abundantes.

Table of contentes:

Abbreviations

CVC	Critical vesicle concentration
DNA	Deoxyribonucleic Acid
DODAB	Dioctadecyldimethylammonium Bromide
DPH	1,6-diphenyl-1,3,5-hexatriene
DLS	Dynamic Light Scattering
EE	Encapsulation efficiency
GFP	Geen fluorescent protein
HDL	High density lipoproteins
HEPES	4-(2-hydroxyethyl) -1-piperazineethanesulfonic acid
has	Human Serum Albumin
Kp	Partition Coefficient
LDL	Low-density lipoproteins
LUVs	Large Unilamellar Vesicles
MLVs	Multilamellar Vesicles
MO	Monoolein (1-oleoyl-rac-glycerol)
PdI	Polydispersity Index
RL	Loading Content
ROS	Reactive Oxygen Species
RSV	Resveratrol
SIRT1	Sirtuina 1
SC	Synthetic complete medium
SD	Standard Deviation
T_m	Main Phase Transition Temperature
UV	Ultraviolet
VIS	Visible
YPD	Yeast extract peptone dextrose

Figures Index

Table

Equation Index:

Introduction to the thesis format

The content of this thesis is written in a form of a manuscript

Title: Internalization of resveratrol nanoparticles in yeast and bioactivity, Célia Barbosa, Inês Ferreira, Viviana Martins, Cátia Pereira, Marlene Lúcio, Manuela Côrte-Real, M. Elisabete C.D. Real Oliveira and Hernâni Gerós (manuscript in preparation)

Author contributions: HG, MECDRO, MCR and ML raised the hypothesis underlying this work. CB, IF, VM, CP and ML performed the experiments. IF and CB prepared and characterized RSV-loaded nanoformulations. CB and IF studied the internalization of RSV-loaded liposomes by yeast cells and the effect of free and RSV-loaded nanoformulations on oxidative stress, and CB studied the effect of RSV on mitochondrial dynamics in yeast cells. CB, IF, VM, CP and ML analysed the data. CB and IF prepared the first draft of the manuscript. HG, MECDRO and ML revised the paper. HG and MECDRO directed the study.

1. Introduction

1.1 Natural phenolic compounds and the French paradox

Natural phenolic compounds represent the major group of phytochemicals with antioxidative properties found in plants, particularly in fruits, seeds and leaves, and its derivative foods and drinks, including chocolate, tea and wine[1,2]. These are a class of phenylalanine-derived chemical compounds with a reactive hydroxyl group (-OH) bonded directly to an aromatic hydrocarbon ring. They are classified as simple phenols or polyphenols according to the number of phenol units[3,4].

The consumption of red wine has been associated to the so-called 'French paradox' a term coined to describe the observation that the French population has a very low incidence of cardiovascular disease, despite a diet high in saturated fat[5,6,7]. The polyphenol resveratrol (RSV; Figure 1) has been pointed out as the main contributor to the cardiovascular protection[5,8]. The benefic cardiovascular effect of RSV can, in turn, be related with its proved capacity to act as a modulator of the metabolism of lipoproteins[9,5] inhibiting the oxidation of low-density lipoproteins (LDL), and inhibiting either platelet aggregation or proatherogenic eicosanoids production by human platelets and neutrophils[5]. Consequently, RSV is responsible for increasing high density lipoproteins (HDL) that take part on the cholesterol removal from atheroma preventing the obstruction of the arteries[10].
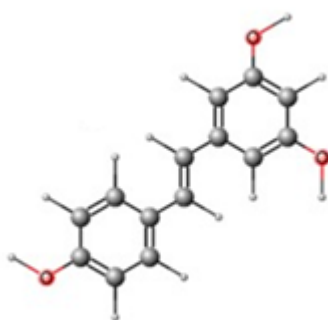
Figure 1. Chemical structure of resveratrol. The chemical structure was drawn using MarvinSketch® software from Chemaxon®. Gray spheres are carbons, white spheres are hydrogens and red spheres are oxygens.

1.2 Beneficial effects of resveratrol and bioavailability

In addition to the above mentioned cardiovascular benefic actions, RSV may protect diabetic patients from meal-induced oxidative stress[11], and several other pharmacological effects have been attributed to this compound, including antibiotic and chemopreventive properties[9,5,12,13,14]. Different

studies on the resveratrol bioavailability after oral ingestion and clinical trials have been conducted both in rodents and humans[15,7]. Results indicate that the benefic use of RSV as an additive to increase nutritional value is limited by its intrinsic features that lead to low bioavailability and formulation challenges; the most problematic one being the low water-solubility and instability[16]. Indeed, several studies have demonstrated that RSV and other polyphenols have a very low bioavailability, which led to the suspect that many of the beneficial health effects observed in either cells or biochemical assays, may not be achievable in humans due to its rapid metabolism[7].

1.3 Liposomes in drug delivery

In order to improve RSV bioavailability and pharmacokinetic profile, several atempts have been made to encapsulate RSV in lipid nanocarrier systems[17,15,18]. Liposomes are the most clinically established nanocarrier systems for drug delivery[19,20]. They are composed by amphiphilic molecules that, when in aqueous solution and above the critical vesicle concentration (CVC), spontaneously self-assemble into closed lipid bilayers. The control of the structure of the liposomes, namely size and size distribution, membrane morphology and supramolecular organization, is important so they can be applied as drug delivery systems[21,22,23,19,20]. The therapeutic efficiency of the nanocarrier systems is highly dependent on the characteristics of the lipid molecules forming the nanoaggregate, which strongly influence structure and stability of liposomes in physiological conditions. The charge of the polar headgroups determines if liposomes are anionic, cationic, zwitterionic, or non-ionic. Previous work from our group has shown that liposomes prepared with the cationic dioctadecyldimethylammonium bromide (DODAB) and a neutral helper lipid monoolein (MO) at several molar ratios, are promising nanocarriers for nucleic acids delivery[24,25,26,27,28]. The presence of MO on the formulation, at low molar ratio, increases fluidification of the nanocarrier and stabilization of the liposomal structures [24, 25, 26].

In our laboratory, we have developed an efficient encapsulation nanosystem for RSV and some important parameters have been studied to assure a future efficient biological application of the nanosystem[29]. In this regard, a thorough biophysical characterization of the nanosystems was made, namely: (i) size, surface charge and morphology of the nanosystem; (ii) microviscosity and thermodynamic parameters of RSV distribution in the nanosystem; (iii) binding of the nanosystem to plasma proteins, and (iv) predicted RSV release at relevant physiological condition. In this project yeast cells were used as a simple eukaryotic model system to understand the internalization of RSV and its cellular effects[29].

1.4 Yeast as model organism

Saccharomyces cerevisiae is one of the most intensively studied eukaryotic model organism in molecular and cell biology. Basic cellular mechanisms of DNA replication and recombination, cell division and death, metabolism as well as cell response to stress and autophagy are well conserved between yeast and higher eukaryotes, including mammals. For instance, sirtuins which are a class of evolutionary conserved histone deacetylases, were originally identified in yeast, and since then their pathogenetic roles in cancer, diabetes, muscle differentiation, heart failure, neurodegeneration and aging have emerged[30]. Autophagy-related genes were also firstly identified in yeast[31]. Moreover, the complete sequence of *S. cerevisiae* genome has proved to be extremely useful as a reference towards the sequences of human and other higher eukaryotic genes[32]. Furthermore, this budding yeast grows well in culture, is stable as either a diploid or haploid cell type, and is amenable to both classical genetic as well as molecular genetic manipulations. The interest of the yeast model in the study of resveratrol bioactivity emerged from the pioneering work of Howitz and colleagues[33] who identified RSV as a potent SIRT1 activator regulating the longevity of this microorganism. RSV also decreased acetylation-dependent p53 activation and protected human cells from p53-dependent apoptosis. Subsequent studies have shown that RSV is also able to regulate the longevity of worms, flies and in short-lived fish, but the exact role of resveratrol and SIRT1 in longevity is still under debate. Similar to most other polyphenols, RSV is suggested to possess intrinsic anti-oxidant capacity, but it is also able to induce the expression of a number of antioxidant enzymes, which probably contribute to an overall reduction in oxidative stress. RSV further interacts with a large number of receptors, kinases, and other enzymes that could plausibly make a major contribution to its biological effects [7]. More recently, it was shown that RSV can inhibit the proliferation of the fission yeast *Schizosaccharomyces pombe* by regulating gene expression and trigger an extensive metabolomic reprogramming[34].

1.5 Working hypothesis and objectives

Although during the last few decades diferent reports have addressed the biological activities of resveratrol and its metabolization in humans, important gaps of knowledge still persist regarding its mode of action at the cellular level. Also, our understanding on how resveratrol is incorporated into the cells is still puzzling. In the present study we aimed to address the following questions:

(i) are DODAB:MO liposomes adequate and stable delivery systems for RSV?

(ii) are RSV loaded liposomes internalized by yeast cells?

(iii) are RSV-loaded liposomes more efficient in protecting cells from oxidative stress than free RSV by slowing RSV degradation and promoting RSV uptake?

(iv) do RSV-loaded liposomes change mitochondrial dynamics?

To answer the scientific questions above we thoroughly characterized the DODAB:MO formulation with different biophysical methods and studied the internalization of RSV-loaded liposomes by yeast cells with fluorescent probes and fluorescence. We then compared the biological activity of free RSV and RSV-loaded liposomes using the yeast as eukaryotic cell model through the use of ROS-sensitive probe coupled to flow-cytometry analysis. The effect of free RSV and RSV-loaded liposomes on mitochondral dynamics was assessed by fluorescence microscopy in a yeast strain expressing a mitochondrial GFP. Overall, we aimed to fill a gap in the knowledge regarding the improvement of RSV bioavailability and bioactivity through the use of an efficient nanoencapsulation system. To this end a set of biophysical, biochemical and analytical strategies were combined taking advantage of the complementary know-how of the team involved in this work.

2. Materials and Methods

Dioctadecyldimethylammonium bromide (DODAB) (purity > 98.0%), 1-monooleoyl-rac-glycerol (MO) (purity > 99.0%) and resveratrol (RSV) were purchased from Sigma-Aldrich (Bornem, Belgium), and used without further purification. Figure 2 shows the chemical structure of the lipids.
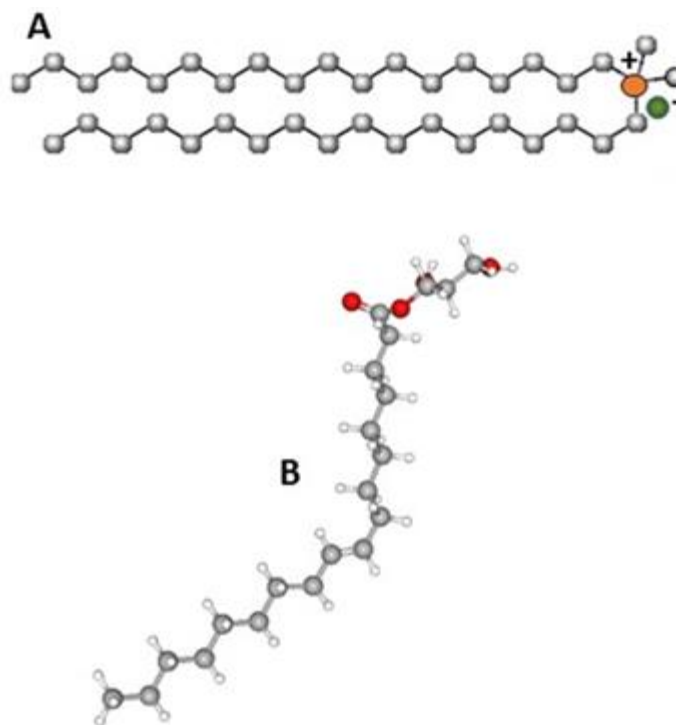
Figure 2. Chemical structures of **(A)** DODAB and **(B)** MO lipids. The chemical structures were drawn using MarvinSketch® software from Chemaxon®. Gray spheres are carbons, white spheres are hydrogens, red spheres are oxygens, orange sphere is nitrogen and green sphere is bromide counter-ion. For sake of simplicity the hydrogens on DODAB were omitted.

2.1 Preparation of lipid formulations

Lipid formulations were prepared with DODAB and the neutral lipid MO by the lipid film hydration method[35]. Briefly, defined volumes of DODAB and MO (20 mM in ethanol) were added to glass tube and the solvent evaporated under nitrogen gas stream until the lipid film was completely dried. Afterwards, the lipid film was hydrated with 10 mL of ultrapure water and the suspension was incubated above the lipids' transition temperature T_m (60° C), alternating with vigorous vortex stirring, in order to remove all the lipid film adsorbed in the glass tube walls. This process lasted for approximately 30 min and resulted in a suspension of large multilamellar vesicles (MLVs) of DODAB:MO (1:2) with a 1 mM final concentration. The MLVs suspension was then repeatedly passed through a Lipex extruder heated to a 60°C temperature and under pressures of 6 bar. The

suspension was passed through Nuclepore Track-Etched polycarbonate membrane filters with different pore diameters (400, 200 and 100 nm) to obtain small and homogeneous large unilamellar vesicles (LUVs). The lipid formulations obtained were then stored at 4°C for further shelf stability studies.

2.2 Preparation of lipid formulations loaded with resveratrol

Lipid formulations were loaded with RSV by the incubation method to obtain final RSV concentrations of 100 or 200 μM and final lipid formulation concentration of 1 mM. An appropriate amount of an ethanolic solution of RSV was added to a glass tube and the solvent evaporated under nitrogen gas stream. LUVs prepared by the above described method where added to the flask containing the dried film of RSV. Finally, the mixture of lipid formulation and resveratrol was incubated above the lipids transition temperature T_m (60° C), alternating with vigorous vortex stirring, in order to remove all the bioactive compound adsorbed in the glass tube walls. This incubation procedure lasted approximately 30 minutes to assure the maximum loading of the lipid formulation. Before any experiment, RSV-loaded formulations were separated from unloaded free RSV (see below).

2.3 Preparation of labelled lipid formulations

Labelled lipid formulations were prepared by evaporation to dryness of the lipids' ethanolic solutions of DODAB and MO, mixed with the ethanolic solution of the fluorescent probe 1,6-diphenyl-1,3,5-hexatriene (DPH). The lipid:probe ratio was kept as 100:1 to prevent changes in the structure of the lipid formulation. Labelled liposomal suspensions were protected from light in every steps of their use. The resultant dried lipid film was dispersed with ultrapure water and the subsequent steps followed the lipid film hydration method already described.

2.4 Separation of free and incorporated RSV, determination of encapsulation efficiency and loading content

The lipid nanocarriers previously obtained were centrifuged (Jouan BR4i, Multifunction centrifuge) through centrifugal filter units (Amicon Ultra-4, PLGC Ultracel-PL Membrane, 10 kDa, Milipore) at 3000 rpm at 25° C for 10 min or until complete separation between the nanosuspensions (pellet retained in the filter unit) and the aqueous phase (supernatant). The supernatant containing the dissolved free resveratrol was analyzed in the PerkinElmer Lambda 45 UV/VIS Spectrometer. Spectra were taken in the range of 220-500 nm. Considering the initial

concentration of RSV used in the formulation ([Resveratrol]$_{total}$) and subtracting the free RSV concentration present in the supernatant (concentration of RSV that was not incorporated in the formulation), it is possible to obtain the concentration of RSV that was incorporated in the formulation ([Resveratrol]$_{loaded}$) and thus determine the encapsulation efficiency (EE (%)) by Equation (1):

$$EE\ (\%) = \frac{[Resveratrol]_{loaded}}{[Resveratrol]_{total}} \times 100 \qquad (1)$$

The RSV loading content (RL (%)) was also calculated by the following Equation (2):

$$RL\ (\%) = \frac{[Resveratrol]_{loaded}}{[Lipid\ formulation]} \times 100 \qquad (2)$$

Where [lipid formulation] was the concentration of DODAB:MO (1:2) formulation.

Both EE (%) and RL (%) were calculated for different initial concentrations of RSV: 5, 40, 60, 100 and 200 μM.

2.5 Physicochemical characterization of RSV loaded nanoformulations

2.5.1 Evaluation of size

Nanocarriers' size and distribution was determined by dynamic light scattering (DLS) with a Zetasizer Nano ZS laser scattering device (Malvern Instruments Ltd., Malvern, UK). This technique measures the size of particles dispersed in a medium by the scattering pattern of a laser (4mW He-Ne, 633 nm) passing through the medium. The size calculations assume the presence of spherical particles. Therefore, percent volume distributions assume the volumes of spheres. The samples were analyzed in a water medium and the available software was used to correlate the intensity of scattered light (at a backscattering angle of 173° C) with the hydrodynamic radius of the spherical particle. For each sample, the mean diameter ± SD of three determinations was calculated applying multimodal analysis. Values reported are the mean diameter ± SD for three replicate samples.

2.5.2 Surface charge

The electrophoretic mobility of the nanocarriers, and ultimately their surface charge were evaluated in a Zetasizer Nano ZS (Malvern Instruments Ltd., Malvern, UK) and related with the zeta potential. The samples, diluted with double-deionised water (condutivity less than 0.1μS cm^{-1}), were placed in polystyrene cuvettes with platinum electrodes and then an electric field across the

lipid formulation dispersion was applied. Surface charged nanocarriers within the dispersion migrated toward the electrode of opposite charge and the velocity of particles migration was converted in zeta potential values by using the Smoluchowski's equation. The zeta potential results reported are the mean of three runs from three independent determinations.

2.5.3 Analysis of the morphology

Morphological evaluation of the nanocarriers was performed using Scanning Electron Microscopy (SEM). For SEM analysis, the samples were mounted on conductive carbon adhesive attached to aluminum stubs. The samples were then coated with platinum under vacuum in a sputter coater after which they were visualized with a FEI Quanta 400 FEG scanning electron microscope at CEMUP facilities.

2.5.4 Shelf stability

The long-term stability of a drug product containing lipids can be highly affected by the lipid species used in the formulation. In a general way, the more unsaturated a compound, the easier the product is oxidized, and thus the shorter the shelf life of the product. On the other hand, saturated lipids, such as DODAB, and monounsaturated lipids, such as MO, offer the greatest stability in terms oxidation. With the purpose of assessing the different lipid formulations in terms of shelf stability, parameters such as surface charge and polidispersity were measured up to 84 days. These measurements were performed mainly to assess if the lipid nanocarriers were suffering from membrane rupture, aggregation or sedimentation, and how the resveratrol encapsulation was influencing the stability of the lipid formulation. The surface charge of the lipid nanocarriers and RSV loaded lipid nanocarriers was assessed by zeta potential measurements.

2.6 Biophysical characterization of the formulations

2.6.1 Biophysical and thermodynamic effects of loaded RSV

With the purpose of understanding how RSV impacts membrane biophysical properties such as the transition temperature (T_m) and phase transition cooperativity (B), a lipid formulation of DODAB:MO (1:2) with a 6 mM unloaded and loaded with RSV (0.7%) was prepared as previously described. An 1 mL aliquot of the formulation DODAB:MO (1:2) with and without RSV was placed in a disposable polystyrene cell and the measurements were performed in a Zetasizer Nano ZS (Malvern Instruments) employing the DLS technique. The position of the detector was at 173° C

relative to the laser source (backscatter detection). A first optimization stage was performed, where cell position and attenuator settings for the cell, sample, and measurement type were determined by the default software that adjusts these values based on the sample optical properties, such as turbidity. This step was repeated five times in order to achieve accurate reproducibility in the intensity of the scattered light. These parameters were then introduced and locked manually for the second stage of the experiment. In this second stage, software was used in trend mode which allows multiple measurements to be made over a range of temperatures, being the initial temperature defined to 25° C and the final temperature defined to 60° C, since the phase transition temperatures of both lipids composing the formulation are contained within this range of temperatures. The temperature interval was defined to 1° C and the number of measurements made at each step after equilibration time was 3. Data were collected as "mean count rate versus temperature" and treated with a modified Boltzmann regression curve (Equation 3), presented below:

$$CR = b_{L1} + m_{L1}T + \frac{b_{L2} - b_{L1} + m_{L2}T - m_{L1}T}{1 + 10^{B(\frac{1}{T} - \frac{1}{Tm})}} \qquad (3)$$

where CR represents the average count rate, b_{L1} and b_{L2} represent the y intercept of the straight lines before (b_{L1}) and after (b_{L2}) the phase transition, m_{L1} and m_{L2} represent the slope of the straight lines before (m_{L1}) and after (m_{L2}) the phase transition, T represents the absolute temperature within the cell, B represents the phase transition cooperativity of the system and T_m represents the main phase transition temperature of the system (transition from the gel phase to the liquid-crystalline phase).

The partition coefficient (K_p) of RSV between lipid formulation and aqueous phase (ultrapure water) was determined by derivative spectroscopy in a previous work of the research group[29]. Briefly, samples of LUVs of DODAB:MO (1:2) with increasing concentrations (up to 2000 µM) and a fixed concentration of RSV (40 µM) were prepared. The respective reference of lipid suspensions was prepared in the same conditions, but in the absence of RSV. All samples were incubated at 37° C during 30 min. A SpectraMax Plus 383 ultraviolet-visible plate reader (Molecular Devices) was used to obtain the absorbance spectra of samples and references in the range of 220 nm to 500 nm at physiological temperature (37° C). The references' absorption spectra were subtracted from the samples' absorption spectra and derivation was applied to eliminate the light scattering caused by the presence of lipid formulations. Derivative spectra were calculated using the Savitzky– Golay method in which a second-order polynomial convolution of 13 points was employed. The determination of the partition coefficient from the derivative spectra at the wavelength where the

scattering was eliminated, was made by fitting equation 4 to the experimental data (D versus [L]) using a nonlinear least-squares regression method, where the adjustable parameter is the partition constant, K_p:

$$D = D_W + \frac{(D_M - D_W) K_P [L] V\emptyset}{1 + K_P [L] V\emptyset} \quad \text{where,} \quad D = \frac{\partial^N ABS}{\partial^N \lambda} \quad (4)$$

In this equation, D is the derivative intensity obtained from the absorbance values of the total amount of RSV; DM is RSV distributed on the lipid membrane phase and DW is RSV distributed in the aqueous phase. [L] represents the lipid concentration (in Molar) and V$\emptyset$ is the lipid molar volume.

Kp of RSV in the biphasic system lipid formulation/aqueous media was evaluated at different temperatures (21° C, 24° C, 29° C, 36° C and 41° C). The Van't Hoff analysis of the temperature dependence of Kp values are used to calculate the variation of enthalpy (ΔH) and entropy (ΔS) involved in RSV partition which were determined from the slope and interception of the Van't Hoff linear plot described by the following equation:

$$\ln (Kp) = -\frac{\Delta H}{RT} + \frac{\Delta S}{R} \quad (5)$$

Where R is the ideal gas constant (8.314 Jmol^{-1} K^{-1}) and T is the temperature in kelvin (K). The Gibbs free energy of partition was calculated by the well-known relation:

$$\Delta G = \Delta H - T\Delta S \quad (6)$$

2.7 Serum protein binding

After preparation of lipid formulations as described different sets of samples were prepared: (i) 20 µM RSV loaded lipid formulations with increasing lipid concentrations (10, 50, 100, 500, 1000 and 1500 µM) with 9 µM HSA; (ii) Unloaded lipid formulations with increasing lipid concentrations (10, 50, 100, 500, 1000 and 1500 µM) with 9 µM HSA. The samples were incubated at 37° C and the surface charge of the resultant lipid-HAS aggregates were made by electrophoretic light scaterring in the Zetasizer Nano ZS with an equilibration time of 60 s. The data were treated using the Zetasizer software and GraphPad prism 5[29].

2.8 *In vitro* RSV release

To assess the RSV release from the DODAB:MO (1:2) lipid formulations in physiological conditions, RSV loaded nanocarriers (20%, i.e. 200 μM) were prepared as described. The lipid formulations were maintained in a 50 ml Falcon tube, with either HEPES buffer, pH of 7.4, or acetate buffer, pH 5.0, at 37° C. The lipid formulations were produced with a lipid concentration of 2 mM and then diluted in buffer in a 1:1 ratio. The time points selected to assess the drug release were 0, 1, 2, 3, 4, 5, 22, 24, 28, 45 and 46 h. At each time point 1.5 mL aliquot was placed in an amicon centrifugal filter unit (10 kDa) and the protocol followed was the same as the one described in 2.4.

2.9 Effect of RSV in yeast cell growth

Saccharomyces cerevisiae W303-1A was used to compare the biological effect of free and encapsulated RSV. This strain possesses an ybp1-1 mutation which abolishes Ybp1p function, increasing the yeast sensitivity to oxidative stress[36]. Yeast growth was tested in YPD medium (1% yeast extract, 1% peptone and 2% glucose) in the absence of either RSV or liposomes (control), and in the presence of free RSV (100 and 200 μM), empty liposomes (DODAB:MO; 1:2), or RSV-loaded liposomes (with 100 and 200 μM RSV). The optical density O.D. $_{640nm}$ was recorded at specific time points, during 28 hours to monitor yeast growth.

2.9.1 Analysis of the internalization of RSV-loaded liposomes by yeast cells

To assess if RSV-loaded liposomes were internalized by yeast cells, liposomes were labelled with the fluorescent dye DPH which is used for structural and dynamic studies of hydrophobic regions in biological membranes[37,38]. Liposomes were prepared as described previously in the presence of DPH (3 μM), and the suspension was protected from exposure to light to prevent the probe degradation. When *S. cerevisiae W303-1A* cells reached, the exponential grow phase the liposomes were added at 1:1 liposome/cell suspension ratio. The resulting mixture was incubated at 30° C with shaking (200 rpm) for 4 h. All cultures were protected from light. The following samples were analysed: yeast cells + free DPH; yeast cells + DPH-labelled DODAB:MO (1:2) liposomes; yeast cells + DPH-labelled DODAB:MO (1:2) liposomes and 100 μM RSV; yeast cells + DPH-labelled DODAB:MO (1:2) liposomes and 200 μM RSV. Fluorescence microscopy analysis of the samples was performed at time points 0, 5, 18, 23, 40 and 45 h with a Leica Microsystems

DM-5000B epifluorescence microscope with appropriate filter configurations for DPH. The images were acquired with a Leica DCF350FX digital camera and processed with LAS LEICA Microsystems software. To further confirm that DPH was indeed loaded within the liposomes inside the cells, 50 µl of sample were co-incubated with 1 mM of fluorescent probe FM1-43, which is widely used to label cell membranes and lipid bodies, and the mixture was incubated for 15 min and observed at the fluorescence microscope.

2.9.2 Effect of RSV on cell viability

Fluorescein diacetate (FDA) is an acetoxymethyl ester derivative of fluorescein that has been extensively used as a cell viability and metabolic activity probe. This cell-permeant esterase substrate is a non-polar compound that is taken up by cells by passive diffusion, and once within the cell, it is hydrolyzed to fluorescein by non-specific esterases[39]. Fluorescein, due to its a polar nature, is not eliminated from the cell as quickly as its ester form, which results in intracellular fluorescein accumulation, and so the viable cells appear fluorescent. Therefore, this viability probe measures both enzymatic activity and cell-membrane integrity, which are required to produce and retain the fluorescent product inside the cell, respectively. In order to evaluate the cell viability of yeast cells by flow cytometry, the following mixtures were prepared: yeast cells alone (control); yeast cells + 200 µM free RSV; yeast cells + DODAB:MO (1:2) liposomes with 200 µM RSV (encapsulated RSV). After incubation at 30° C during 12-16 h, samples were centrifuged at 5000 rpm during 2 min and the resulting pellet was resuspended in 1 mL of PBS buffer (pH 7.4, NaCl 137 mM, KCl 2.7 mM, phosphate 10 mM) containing 4 µg/mL of the FDA probe. Flow cytometry analysis of each sample was performed 20 min after incubation with the probe.

2.9.3 Effect of RSV on endogenous ROS production

Dihydroethidium (DHE) is a reduced form of the commonly used DNA dye ethidium bromide. DHE itself exhibits blue fluorescence in the cytoplasm and it has been widely used to evaluate ROS production, since it has the ability to freely permeate cell membranes and, upon reaction with superoxide anions, forms a red fluorescent product (2-hydroxyethidium) that intercalates with DNA. This fluorescent probe detects essentially superoxide anion, is retained well by cells, and may even tolerate mild fixation[37]. ROS production was analysed in the following samples: yeast cells alone (control); yeast cells + 200 µM free RSV; yeast cells + DODAB:MO (1:2) liposomes with 200 µM RSV (encapsulated RSV). Briefly, after incubation at 30° C during 12-16 h, samples were centrifuged at 5000 rpm during 2 min and the resulting pellet was resuspended in 1 mL of PBS

containing 5 μg/mL of the ROS-sensitive probe DHE. Flow cytometry analysis of each sample was performed 30 min after incubation with the probe[29].

2.9.3.1 Effect of RSV in H_2O_2-induced intracellular ROS accumulation

In order to analyse the effect of free or encapsulated RSV in H_2O_2-induced ROS accumulation, mid-exponential phase yeast cells were grown in the absence or presence of 7 mM H_2O_2 and then stained with the 2',7'-dichlorodihydrofluorescein diacetate (H_2DCFDA) probe. This probe is cell-permeable, is hydrolysed by cellular esterases to H_2DCF and, in the presence of intracellular ROS, is oxidised resulting in the formation of a fluorescence product – dichlorofluorescein (DCF). An increase in the green fluorescence of this probe indicates an increment in the levels of ROS production[40]. The following samples were prepared: yeast cells (control); yeast cells + 200 μM RSV; yeast cells + DOBAB:MO (1:2) liposomes; yeast cells + DODAB:MO (1:2) liposomes with 200 μM RSV. When cultures reached mid-exponential phase, 5 mL aliquots were transferred to glass tubes in the absence or presence of 7 mM H_2O_2. H_2DCFDA probe was added at a final concentration of 0.05 mM to 500μL culture sample with an optical density O.D. of 0.1 and incubated for 1 h. Samples were analysed by flow cytometry immediately after H_2O_2 addition and after 24 h.

2.9.3.2 Effect of resveratrol on mitochondrial dynamics

To study the effect of RSV in yeast mitochondrial morphology, the strain *S. cerevisiae W303-1A* Pyx232-mtGFP was used. This strain expresses a mitochondrial matrix-targeted GFP [41]. Cells were grown in synthetic-complete medium (0.67% YNB, 0.14% Drop-out Medium Supplement, 0.008% Histidine, 0.4% Leucine and 0.008% Uracil, 2% glucose and 0.5% ammonium sulphate), in the absence or presence of 100 μM and 200 μM either free or encapsulated, as follows: yeast cells (control); yeast cells + 100 μM RSV; yeast cells + 200 μM RSV; yeast cells + DODAB:MO (1:2) liposomes; yeast cells + DODAB:MO (1:2) liposomes with 100 μM RSV; yeast cells + DODAB:MO (1:2) liposomes with 200 μM RSV. Culture samples were observed at specific time points in Leica Microsystems DM-500B fluorescence microscope with the appropriate filter configurations for GFP. The images were acquired with a Leica DCF350FX digital camera and processed with LAS LEICA Microsystems software.

3. Results

3.1 Characterization of RSV-loaded nanoformulations

DODAB:MO (1:2) nanoparticles are sphere-like with an average diameter size of 130 nm and smooth surface (Figure 3A, B), while RSV loaded nanoformulations are 30-50 nm larger (Figure 3A). The small values of polydispersity of the nanoparticles (0.12-0.18) suggest a fairly narrow and monomodal nanocarrier size distribution for all formulations (Figure 3A).
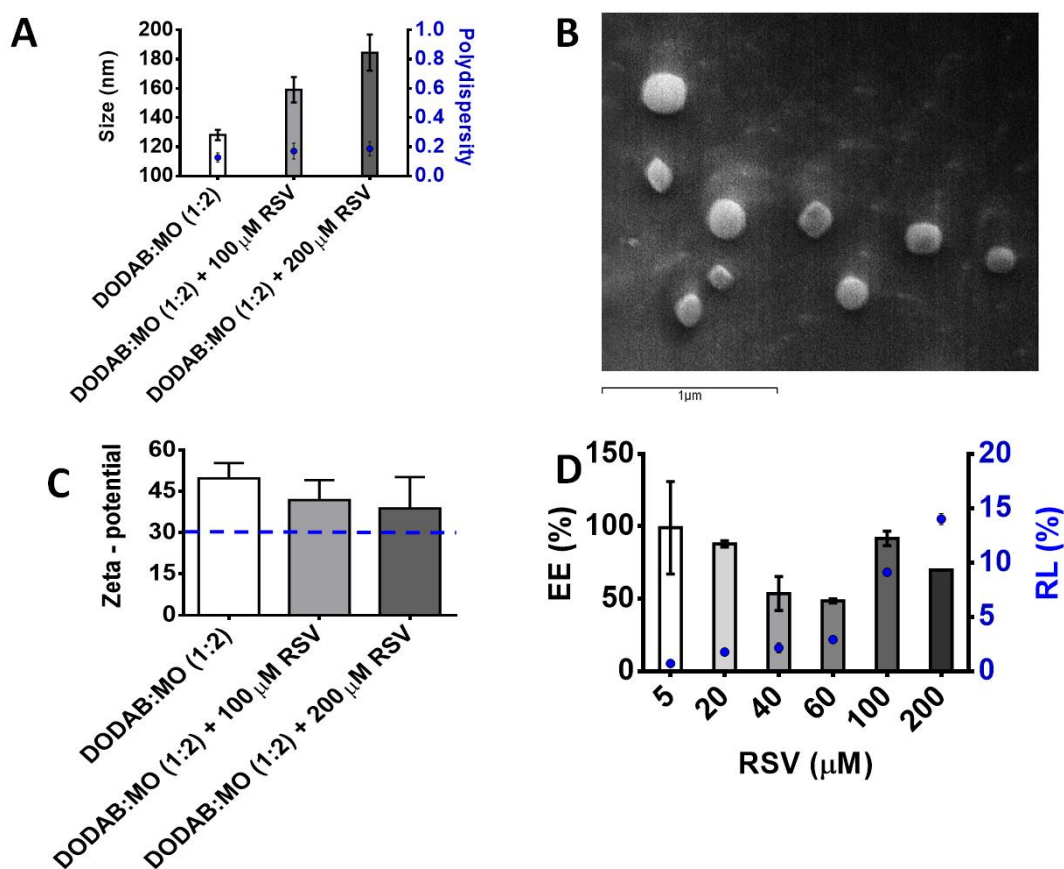

Figure 3.Characterization of RSV-loaded nanoformulations (A) Size distribution (in intensity) of DODAB:MO (1:2) formulations (bars) unloaded and loaded with resveratrol (RSV); and its polydispersity (blue dots). (B) Cryo-SEM images of DODAB:MO (1:2) formulations. (C) ζ-potential values of DODAB:MO (1:2) formulations unloaded and loaded with resveratrol (RSV). The dashed blue line represents the threshold of +30 mV, as minimal value for formulation stability. (D) Encapsulation efficiency (EE%) (bars) and Loading efficiency (RL%) (blue dots) of increasing concentrations of resveratrol (5, 20, 40, 60, 100 and 200 μM) to a 1 mM lipid concentration. Values reported are the mean diameter ± standard deviation for three replicate samples. Results from Inês Ferreira (29) complemented by Célia Barbosa in the present study (A, C and D).

As anticipated, all lipid formulations present a highly positive surface charge owing to the presence of the positively charged lipid DODAB. The ζ-potential of the unloaded formulations (+ 49.7 ± 5.6 mV) is higher than the value of RSV loaded formulations (Figure 3C), most likely because

the neutral RSV molecule is located near the positive DODAB polar headgroups, which decreases the density of positive charges, thus reducing the surface charge of the nanoparticle.

The encapsulation (EE%) and loading (RL%) efficiencies of RSV in the lipid formulations are show in Figure 3D. EE % was above 70% for incubation with 200 μM RSV. Furthermore, up to 200 μM RSV, RL increases with increasing RSV concentration, concentration reaching 14%.

The shelf stability of the nanosystems was evaluated during 84 days at 4.0° C. Only after the first month of storage the ζ-potential decreased to values below the desired +30 mV (Figure 4)
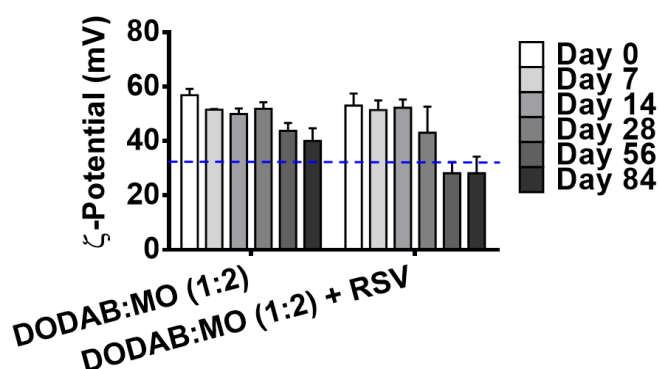

Figure 4. Shelf stabilityζ-potential measurements of DODAB:MO (1:2) formulations unloaded and loaded with 2% (20 μM) resveratrol during the three months following formulation production. **Results from Inês Ferreira (29)**.

In order to calculate the thermodynamic parameters associated with the partition of RSV in a biphasic system DODAB:MO (1:2)/water, the value of partition coefficient (Kp) was determined from 30° C to 60° C. The nonlinear regression fittings of the third derivative values at different temperatures, obtained according Equation 4, are presented in Figure 5A.

RSV shows a high partition coefficient into the biphasic system DODAB:MO (1:2)/water (LogKp = 3.37 ± 0.10). The application of the Van't Hoff linear fitting (Equation 5) to the experimental data and of equation 6 allowed the determination of the enthalpy (ΔH) and entropy (ΔS) variation and free Gibb's energy (ΔG) of RSV partitioning. RSV partitioning in DODAB:MO (1:2) vesicles/water biphasic system at 37° C is associated with ΔH>0 (6.00 ± 0.68 KJ.mol^{-1}) and a ΔS>0 (0.20 ± 0.005 KJ.mol^{-1})[29].

The effect of RSV on the biophysical properties of the lipid membranes was evaluated by DLS assays. The results of the average count rate obtained with lipid nanosystems empty or loaded with RSV are shown in Figure 5B. The data were fitted by Equation 3 to determine the values of phase transition temperature (T_m) and the cooperativity (B) of the transition of the lipid bilayers from the gel phase to the fluid phase (Table 1).
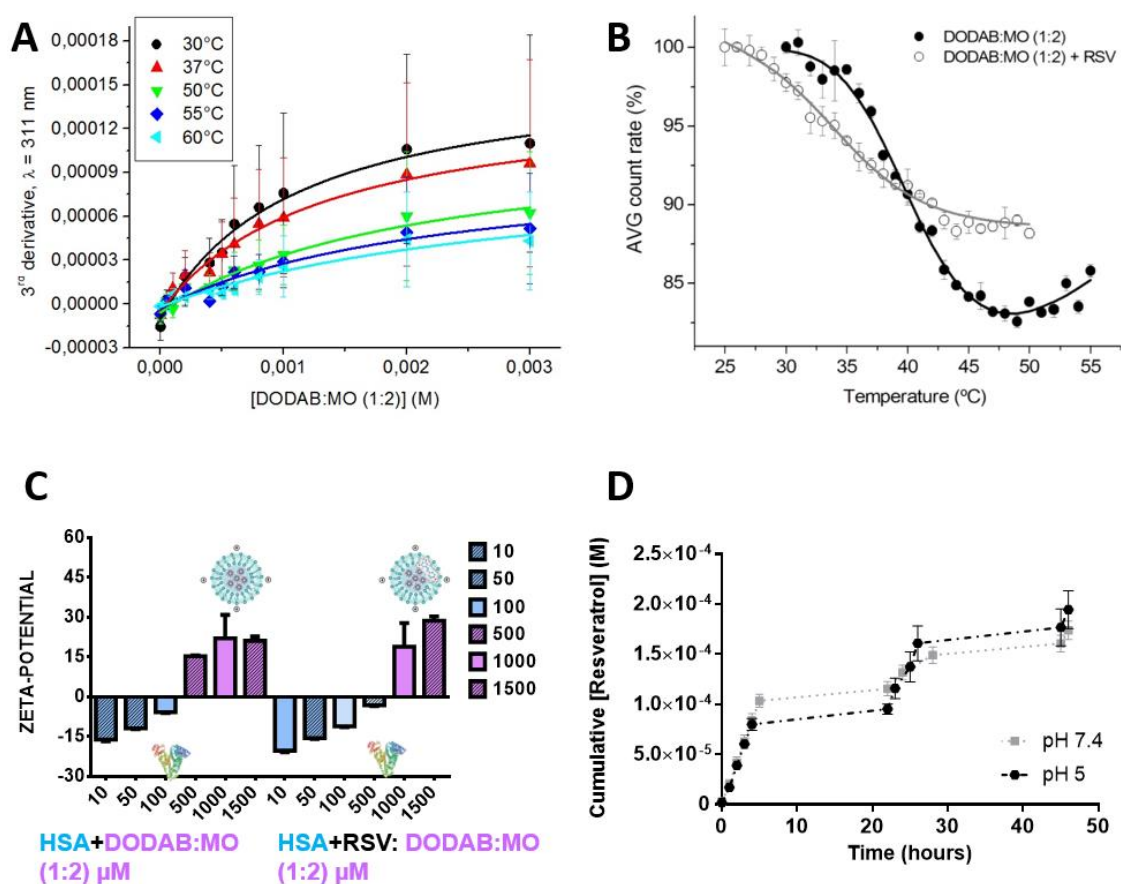
Figure 5. Biophysical properties of the lipid membranes **(A)** Normalized third derivative absorbance spectra at $\lambda= 256$ nm with increasing DODAB:MO (1:2) concentration for the determination of Kp of resveratrol in the biphasic system lipid/water at several temperatures: 30° C (●); 37° C (▲); 50° C (▼); 55° C (◆) and 60° C ( ). Continuous lines are the best fitted curves according to eq 4. **(B)** Normalized average count rate of DODAB:MO (1:2) lipid vesicles unloaded (●) and loaded with resveratrol 20 μM (○)(RSV) as a function of temperature. Continuous lines are the best fitted curves according to eq 3. **(C)** ζ-potential variation of unloaded and resveratrol 20 μM (RSV) loaded lipid formulations DODAB:MO (1:2) with increasing lipid concentrations in the presence of human serum albumin (HSA). * In **(A)**, **(C)** and **(D)**, Values reported are the mean diameter ± standard deviation for three replicate samples. Results from Inês Ferreira (29).

As can be seen in Figure 5C, both unloaded and RSV loaded formulations suffer an inversion of its ζ-potential in the presence of human serum albumin (HSA). However the ζ-potential inversion occurs at higher DODAB:MO (1:2) concentrations, when the nanosystems are loaded with RSV. As shown in Figure 5D the lipid formulations allow a controlled release of RSV over a period of almost 50 h, which is not substantially affected by the pH value, from pH 5 – 7.4.

Table 1. Biophysical parameters (B and T_m) of DODAB:MO (1:2) liposomes in the absence and presence of resveratrol (20μM)[29].

	B (cooperativity)	T_m (°C)
DODAB:MO (1:2)	217 ± 58	41.7 ± 1.0
DODAB:MO (1:2) + 20 μM RSV	169 ± 12	36.7 ± 0.3

3.2 Internalization of RSV-loaded liposomes by yeast cells

As reported to in Material and Methods section, RSV- loaded liposomes were labeled with the fluorescent probe DPH to evaluate by fluorescence microscopy the capacity of yeast cells to internalize these nanoparticles. Different studies have shown that DPH permeates into the membrane and this probe, besides being located in the centre of the lipid bilayer, is also capable of entering the cell and of being incorporated into the membranes of the cellular organelles, and into the intracellular lipid droplets. Moreover, the intercalation of DPH into membranes is accompanied by strong fluorescence enhancement because its fluorescence is practically negligible in water[37,38]. As shown in Figure 6A, after 5 h incubation yeast cells readily internalized liposomes, that appeared as bright blue spots in the periphery of the central vacuole. Moreover, when yeast cells were incubated with DPH alone no fluorescence was detected in the cytosol.

When yeast cells were incubated with the lipophilic fluorescent probe FM1-43, results showed that its green fluorescence co-localized with the blue fluorescence of DPH, suggesting that liposomes are efficiently internalized by cells and follow the endocytic pathway.
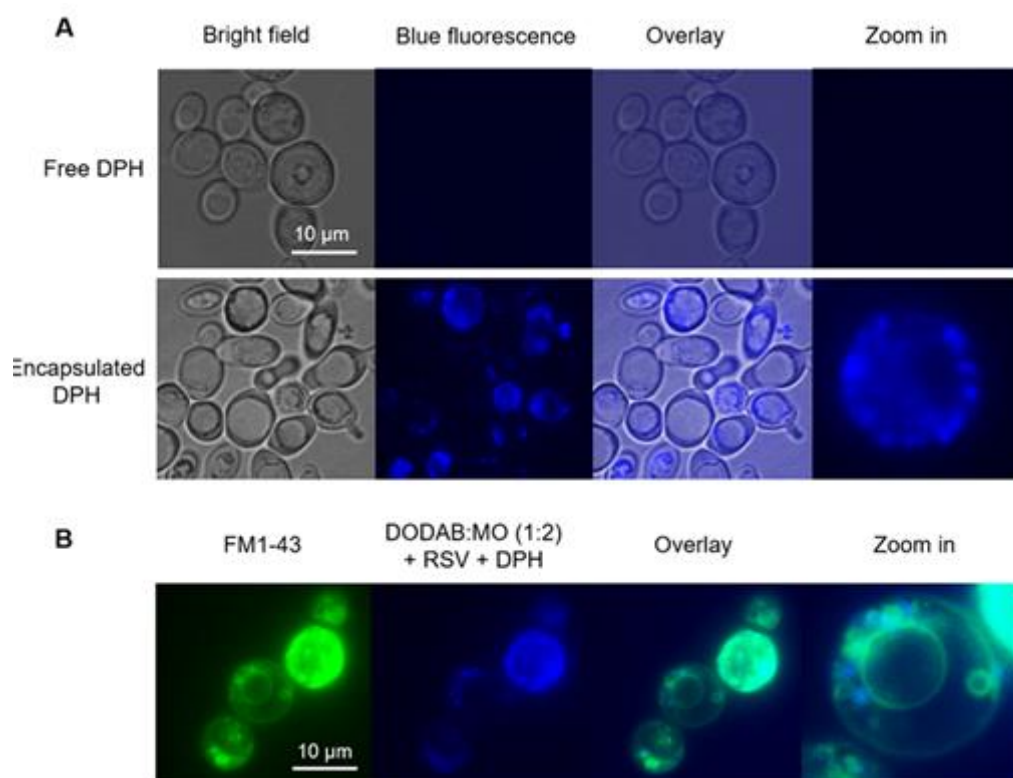
Figure 6. Internalization of resveratrol-loaded liposomes by yeast cells **(A)** *S. cerevisiae* W303 cells were incubated for 4 h with liposomes loaded with resveratrol and with 3 µM free DPH (upper panel), or with liposomes loaded with resveratrol and DPH (encapsulated DPH; lower panel). Images show bright field, blue fluorescence from DPH and the overlay of these two micrographs. **(B)** Yeast cells internalizing DPH-loaded liposomes were incubated with the fluorescent probe FM1-43. Images show green fluorescence (FM1-43), blue fluorescence (DODAB:MO (1:2) + RSV + DPH) and the overlay of these two signals (overlay, zoom in). **Results from Inês Ferreira (29) complemented by Célia Barbosa in the present study (A)**.

3.3 Effect of free and RSV-loaded nanoformulations on oxidative stress and mitochondrial dynamics in yeast cells

Results showed that the growth of *S. cerevisiae* W303 cells in batch cultures in YPD medium up to 28 h was not significantly affected by the presence of 100 and 200 µM free RSV, RSV-loaded liposomes or liposomes alone. Moreover, neither free RSV nor RSV loaded nanoformulations affected cell viability as evaluated by flow cytometry with the fluorescent probe FDA (Figure 7).

To evaluate if the intracellular redox state could be affected, even if transiently, by free RSV or RSV-loaded liposomes, S. cerevisiae W303 cells were labeled with the ROS-sensitive probe DHE and the population was analyzed by flow cytometry. A representative result is presented in Figure 8. The acquisition protocol was defined to measure forward scatter (FS), side scatter (SS), orange fluorescence (FL3) and red fluorescence (FL4) on a logarithmic scale. The scattergram of Figure 8 shows a well-defined population of yeast cells (gated region W). The same gate was defined for all

subsequent experiments and the number of yeast cells was set to 20000. The overlay of the histograms corresponding to the autofluorescence of the yeast cells and the fluorescence of yeast cells labeled with DHE clearly shows a positive staining (Figure 8), suggesting that the probe reacted with intracellular superoxide anion. Results also show that free resveratrol (200 µM RSV) or encapsulated (DODAB:MO (1:2) + 200 µM RSV) promoted a decrease of the fluorescence intensity, and the effect was more pronounced in the latter case (Figure 8).
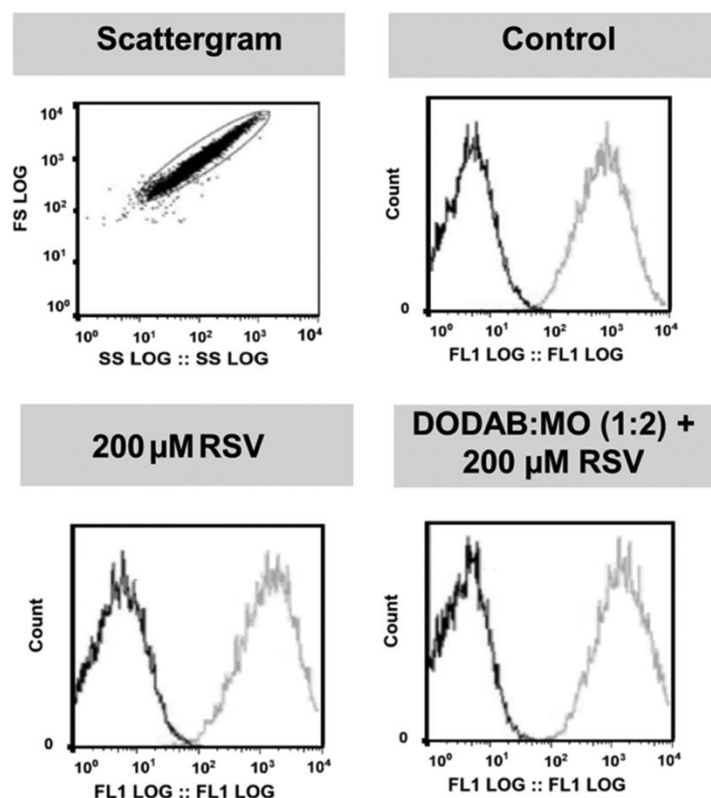
Figure 7. Viability of *S. cerevisiae* W303 cells evaluated by flow cytometry with the FDA probe. The scattergram of the population of yeast cells in the absence of resveratrol is first shown. The overlay histogram of autofluorescence (black line) and FDA fluorescence (grey line) in the absence of resveratrol (Control) and upon treatment of yeast cells with 200 µM of free resveratrol (200 µM RSV) and resveratrol loaded liposomes (DODAB:MO (1:2) + 200 µM RSV) is also. Results from Inês Ferreira (29) reproduced by Célia Barbosa in the present study.
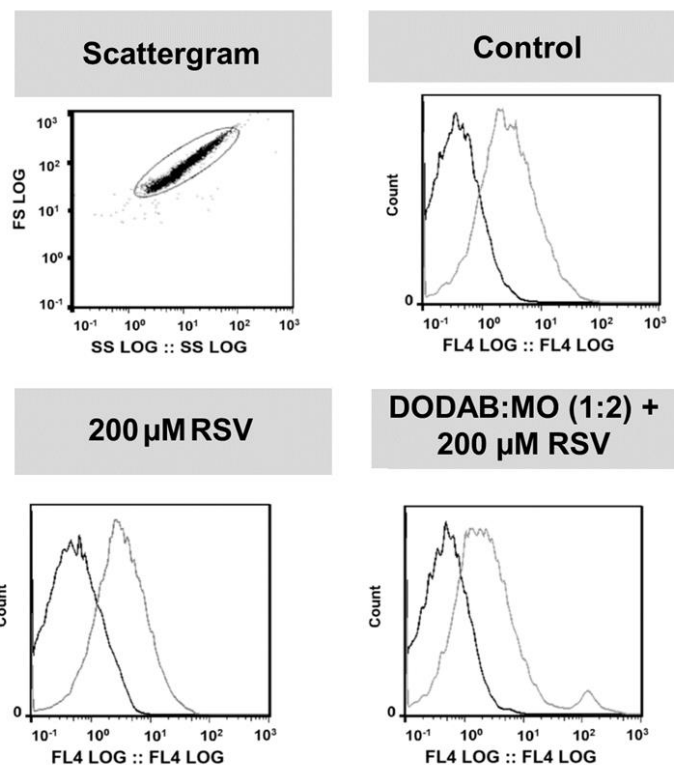
Figure 8. Flow cytometry analysis of *S. cerevisiae* W303 yeast cell populations to study the effect of resveratrol against endogenous ROS with the DHE probe. Scattergram of a population of yeast cells in the absence of resveratrol; overlay histogram of autofluorescence (black line) and DHE induced fluorescence (grey line) in the absence of resveratrol and upon treatment of yeast cells with 200 μM of free resveratrol and resveratrol loaded liposomes. Results from Inês Ferreira (29).

We next investigated the role RSV in response to exposure to the pro-oxidant compound H_2O_2 and determined the accumulation of ROS by staining with dichlodihidrofuorescein diacetate (H_2DCFDA) and flow cytometry analysis (Figure 9) [40]. When yeast cells were incubated with 7 mM H_2O_2, a ca. 4-fold increase in the levels of ROS was observed after 24 h after treatment, which was prevented by 200 μM free RSV. Moreover, unloaded liposomes completely eliminated basal endogenous ROS and protected cells from the ROS induced by H_2O_2. However, RSV loaded liposomes exhibited a strong pro-oxidant effect, leading to a 6-fold increase in the levels of ROS in comparison with unloaded liposomes.
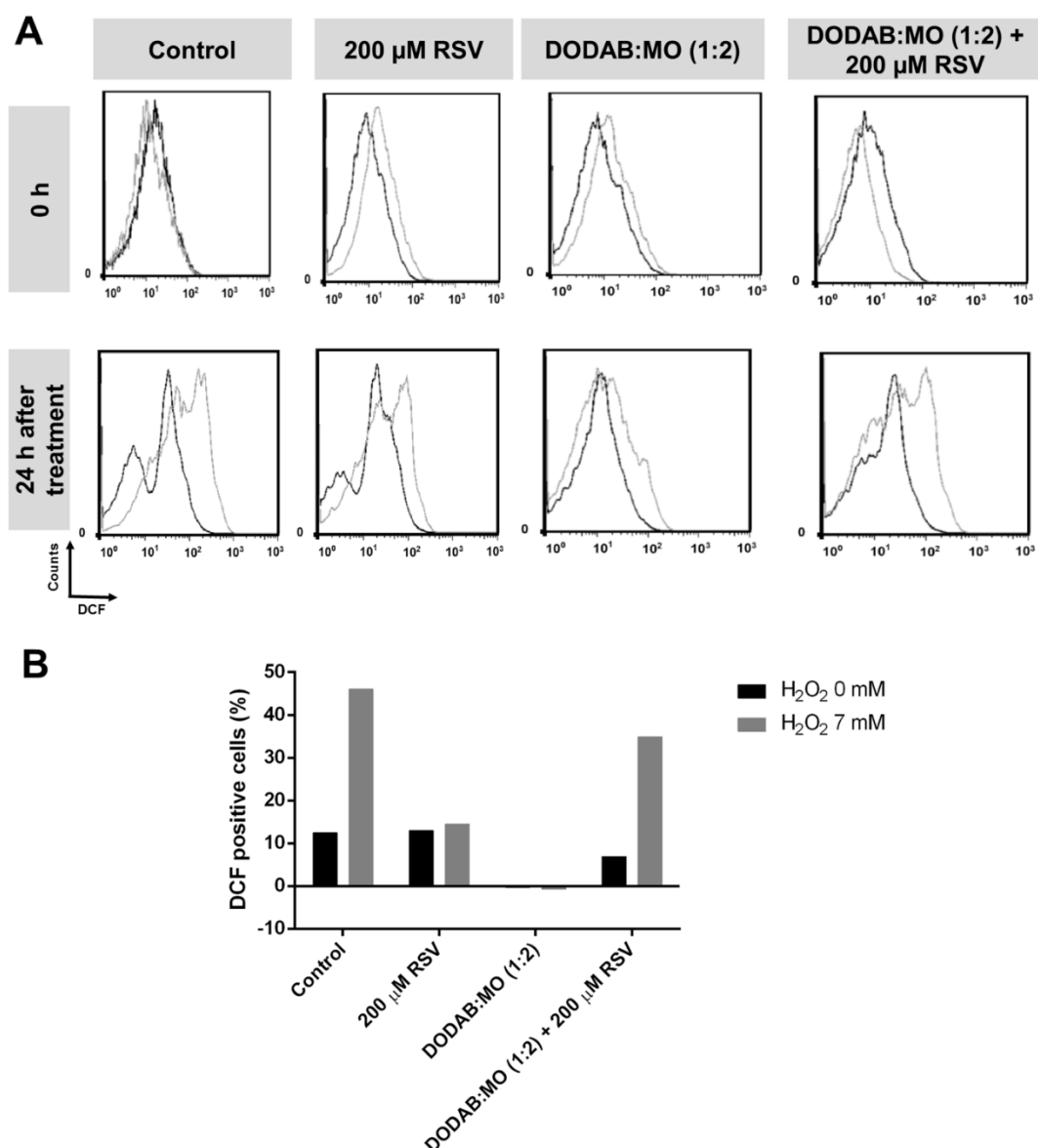
Figure 9. Flow cytometry analysis of intracellular reactive oxygen species (ROS) levels of *S. cerevisiae* W303 cells stained with 2′7′-dichlorofluroescein diacetate (H₂DCFDA). **(A)** Representative histograms of yeast cells incubated in the absence and in the presence of 200 µM resveratrol (200 µM RSV), liposomes (DODAB:MO (1:2)) and liposomes loaded with 200 µM resveratrol (DODAB:MO (1:2) + 200 µM RSV) in the absence (black) or presence (grey) of 7 mM H₂O₂. Histograms from timepoint zero and 24 h after treatment are shown. **(B)** Quantification of the percentage of cells exhibiting positive DCF fluorescence in relation to timepoint zero. The positive fluorescence gate was settled from the autofluorescence of each sample in each timepoint. Results represent the percentage of positive DCF cells at timepoint 24 h subtracted for the positive percentage already present in timepoint zero.

As reported to in the Material and Methods section, to study the effect of RSV in yeast mitochondrial morphology, the strain *S. cerevisiae W303-1A* Pyx232-mtGFP, which expresses a mitochondrial matrix-targeted GFP was used. Representative fluorescence microscopy images of cells in the absence or presence of free or RSV-loaded liposomes are shown in Figure 10. For each

treatment and time point at least 100 cells were analyzed and classified as containing non-fragmented/tubular mitochondrial networks, fragmented mitochondria, or vacuolar/diffuse cytosolic fluorescence indicative of mitochondria internalization and degradation, respectively (Figure 10).
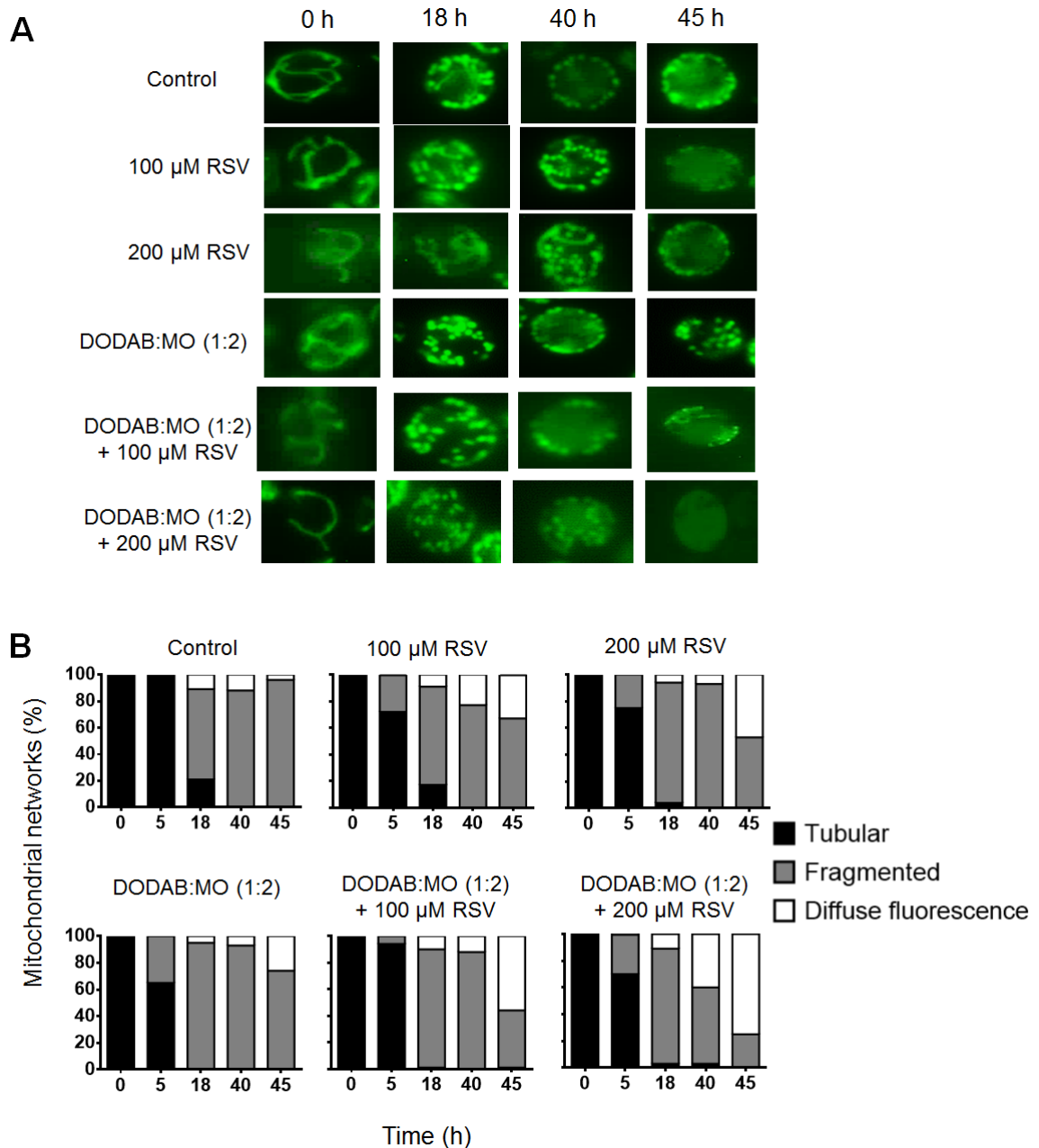
Figure 10. Mitochondrial network morphology in *S. cerevisiae* W303-1A Pyx232-mtGFP cells throughout growth in medium with or without supplementation of free (100 µM RSV, 200 µM RSV) or encapsulated resveratrol (DODAB:MO (1:2) + 100 µM RSV, DODAB:MO (1:2) + 200 µM RSV). The effect of liposomes without RSV was also assessed (DODAB:MO (1:2)). Samples were observed for each condition at specific time points. (**A**) Representative images of mitochondrial networks displaying green fluorescence of Pyx232-mtGFP. (**B**) Proportion of mitochondrial morphologies in 100 cells per condition.

Results clearly show that cells displaying non-fragmented/tubular mitochondrial networks predominate up to 5 h mostly in control conditions, while a the vacuolar/diffuse cytosolic fluorescence predominate after 40 h of incubation either with free or encapsulated RSV. Moreover, the incubation with liposomes containing 200 µM RSV during 45 h was the experimental condition where cells exhibiting the latter phenotype were more abundant.

4. Discussion

4.1 DODAB:MO liposomes are adequate delivery systems for RSV

The liposomal formulations used in this work were composed of DODAB and MO at (1:2) molar ratio. This type of vesicular structure presents simultaneously a structural rigidity of the lipid bilayer caused by DODAB molecules, required for the retention of the encapsulated compound, and also a fluid content, as a consequence of MO which promotes inverted non-lamellar phases at the inner core of the vesicular structure, important for increasing the encapsulation efficiency, as demonstrated for different proteins[42,43]. The MO content also provides the nanosystem with fusogenic properties[28], which might be relevant for an antioxidant therapeutic application[44]. It has been reported that the optimal size of a nano-sized agent to induce efficient therapeutic effect ranges between 100 and 200 nm in diameter, thus above the kidney clearance and below the mononuclear phagocytic system thresholds, which allows the nanocarriers to circulate for prolonged periods of time[45]. Our results, supported previous work[29] suggesting that RSV-loaded liposomes are suitable for resveratrol delivery purposes because the average diameter size of DODAB:MO (1:2) liposomes, either empty or loaded with RSV, is below 200 nm.

Zeta potential values are not quantitatively identical to the surface charge values of the nanocarriers, but are very helpful in the qualitative prediction of the surface charge. The unloaded formulations present a ζ-potential value consistent with the previously obtained values for the same system[28].

RSV loaded formulations show lower ζ-potential values than unloaded formulations most likely because the neutral resveratrol molecule is located near the positive DODAB polar headgroups, which decreases the density of positive charges, thus reducing the surface charge of the nanoparticle.

The common dividing line between stable and unstable particles is usually taken at either +30 mV or -30 mV. Nanoparticles with a large negative or positive surface charge tend to repel each other, which prevents the formation of aggregates. Thus, the observed high surface charge of

DODAB:MO (1:2) liposomes may explain the observed stability, at least until the first month of storage.

The measured high partition coefficient of RSV in the binary system DODAB:MO (1.2)/water suggests that this bioactive compound has a lipophilic character, which facilitates its efficient encapsulation in the lipid formulation, in agreement with the observed high values of encapsulation and loading efficiencies indicative that the system can incorporate high amounts of RSV.

RSV partitioning in DODAB:MO (1:2) vesicles/water biphasic system at 37° C is characterized by a positive ΔH and a positive ΔS, typical of hydrophobic interactions established between RSV and the lipids and ΔG<0 reflecting the spontaneity of the partition process.

From DLS assays it was possible to evaluate the influence of RSV in the microvicosity of the nanosystems. The plain DODAB:MO (1:2) system presents a high cooperativity, which means that all the lipid molecules transit to a different phase practically at the same time. However, when RSV is encapsulated in the same system, its cooperativity is diminished. This decay in the phase transition cooperativity supports that RSV was successfully encapsulated. Also, it indicates that the RSV molecules are somewhat not evenly distributed in the lipid formulation, since the compound is only influencing certain molecules to change their phase transition temperature.

It was also possible to verify a decrease in the phase transition temperature of the system of 5° C in the presence of RSV, when compared to the unloaded lipid formulation. This T_m decrease is a result of a weaker interaction of the headgroup moieties, paralleled by a lateral expansion of the interface region, which indicates that the RSV molecules are located in the most organized portion of the lipid membrane system, within the DODAB polar headgroups and interacting at C1 - C8 level of the lipid acyl chains[46]. Despite being a lipophilic drug, RSV has three hydroxyl (-OH) groups, which need to be embedded in a polar zone. Therefore, RSV decreases lipid nanosystem's microviscosity by insertion at a rigid portion of the vesicle. The interaction of RSV with the lipid membrane of its nanocarrier formulation impacts its ability to protect the body from harmful free radicals in several ways.

The localization of RSV in the lipid formulation affects the availability of this bioactive compound to oxidation radicals. Also, the rate of lipid peroxidation is influenced to a strong degree by the physical state of the membrane in a way that is not completely understood. RSV is shown here to decrease the microviscosity of the lipid acyl chain, which is likely to have the effect of increasing lateral diffusion within the membrane. The increased rates of diffusion will simultaneously increase the rate of propagation of free radicals and cellular membrane peroxidation products that can in this way be accessible to RSV. RSV has a disordering effect on the lipid formulation and binds to the lipids suggesting a mechanism for the enhanced clinical efficiency of loaded RSV formulations[47].

Both unloaded and RSV loaded formulations suffer an inversion of its ζ-potential in the presence of human serum albumin (HSA). When HSA is present in surplus, the ζ-potential is negative because HSA has anionic residues exposed at the surface and there are less positively charged nanosystems. However, as the concentration of nanosystems increases, so does the ζ-potential. Interestingly, RSV loaded nanosystems present a slower inversion of the ζ-potential compared to unloaded nanosystems, which might be caused by the localisation of RSV molecules at the superficial part of the lipid headgroups, thereby reducing the positive surface charge of the vesicles and thus hindering the binding of HSA.

The RSV release profiles from the formulation in two different physiological conditions, namely that which mimics the pH of the bloodstream (pH = 7.4) and the cancerous tissue (pH = 5) are very similar, it was observed that the ionization of resveratrol is not significantly different at the two pH values. According to these profiles it is possible to conclude that the lipid formulation allows a RSV controlled release over periods of almost 50 h.

4.2 *S. cerevisiae* proliferation and viability are not affected by 100 - 200 μM free RSV and resveratrol-loaded liposomes

The effect of RSV on the inhibition of cancer cell growth is relatively well documented[48,49,50,34]. RSV (up to 438 μM) also demonstrated a sustained antibacterial activity against *Propionibacterium acnes*, and a combination of both resveratrol and benzoyl peroxide, the latter commonly used in the treatment of acne, showed high initial antibacterial activity and sustained bacterial growth inhibition[51]. RSV also inhibited the proliferation of the yeast *Schizosaccharomyces pombe* in a dose dependent manner (11- 88 μM) and induced significant changes in the transcriptome and metabolome of this fission yeast[52]. Moreover, as reported to in Introduction, the budding yeast *Saccharomyces cerevisiae* has been used as an eukaryotic model to study the effect of RSV, after the pioneering discovery that RSV is a potent SIRT1 activator regulating the longevity of the microorganism[33]. More recently, it was shown that in *S. cerevisiae,* the effects of RSV are dependent on the cellular energy status and linked to respiration since the resveratrol inhibits cell proliferation, as does when antimycin A (a specific inhibitor of electron transport chain complex III) occurred during the respiratory phase[53]. Accordingly, 1000 μM RSV significantly inhibited cell growth when cells were cultivated in respiratory substrates, like ethanol or glycerol. In a previous study, the same group observed that much lower doses of RSV (30 μM) stimulate glycolysis via the "sucrose non-fermenting 1" gene (SNF1, *S. cerevisiae* orthologous of AMPK) in cells growing in fermenting conditions[54]. The results of the present study are in accordance to those reported before. We observed that 100 – 200 μM free RSV did not change significantly the specific growth rate of *S.*

cerevisiae cultivated in fermenting conditions, and that the slight reduction of the proliferation rates observed in the presence liposomal formulations with distinct RSV content seemed to be due to DODAB:MO formulation per se. Accordingly, our flow cytometry results with the fluorescent probe FDA, suggested that neither 100 – 200 µM RSV alone nor resveratrol loaded liposomes induce loss of cell viability. Thus, a robust effect of RSV on the growth and viability of *S. cerevisiae* is only observable in the milimolar range in cells growing under energy-deprivation or respiratory substrates, and its main intracellular target seems to be the mitochondria, as suggested by Madrigal-Perez et al., (2016) when 10 – 1000 µM RSV completely inhibited cell respiration.

4.3 RSV loaded liposomes are efficiently internalized by yeast cells and protect from oxidative stress

Since RSV has a low water solubility and labile properties and is rapidly metabolised and eliminated in human organism, we exploited herein its encapsulation in DODAB:MO liposomes as a strategy to improve the preservation of its biological properties and enhance its bioavailability. A limited number of studies regarding the interaction of liposomes and yeast cells are available so far. In one of these studies *S. cerevisiae* protoplasts were transfected with liposome-encapsulated plasmid DNA[55], however, the details of these interactions remain obscure. More recently, droplets of essential oils were efficiently encapsulated by yeast cells, but the resolution of the images did not allow further conclusions regarding the mechanisms of encapsulation[16]. Moreover, it was suggested that the loading process of free RSV into yeast cells might occur by passive diffusion boosted by the hydrophobic interactions and H bonds established between the RSV -OH groups and the – NH2, -OH and –COOH groups of the polar headgroups of the phospholipids in the yeast membrane[56]. In the present study, when cells were incubated with RSV loaded liposomes labelled with DPH, the blue fluorescence was very abundant in the cytosol, corroborating previous work[29]. In addition DPH fluorescence clearly co-localized with the green fluorescence of the endocytosis marker FM1-43. Altogether, these observations strongly suggest that a mechanism of endocytosis is involved on the internalization of DODAB:MO liposomes.

Oxidative stress occurs when ROS levels overwhelm the antioxidant capacity of the cells, due to an increase in ROS production, a weakening of the antioxidant systems or both. A previous study has already shown that resveratrol at low doses (5 µM) increase total ROS levels in yeast cells, but 50 µM resveratrol promotes a decrease in total ROS, acting as an antioxidant agent[57]. The same authors showed that ROS accumulation at low RSV levels (5 µM) involves transcriptional changes of the oxidative transcription factor Yap1p gene targets. Many studies also suggest that RSV may act as a prooxidant agent depending on its concentration, time of exposure, and cell

type[58,59]. This dualistic behaviour characterises RSV as an active redox molecule[60]. Indeed, in different cell types, such as a fibroblast cell line and tumour human cells, RSV was found to exert its cytotoxic action at higher doses[61]. Likewise, it was already discussed that RSV induces cell cycle arrest[61,62] and stimulates the reactive oxygen species (ROS)-activated mitochondrial pathway leading to apoptosis[63]. Herein, flow cytometry studies with the ROS-sensitive probe DHE confirmed that 200 µM RSV reduced the intracellular levels of superoxide anion, and the effect was enhanced when RSV was encapsulated into the liposomal formulation. Moreover, when cells were treated with H_2O_2, 200 µM of free RSV showed antioxidant properties, but a pro-oxidant effect of RSV became apparent when 200 µM RSV-loaded liposomes were tested in comparison with unloaded liposomes which exhibited. Nevertheless 200 µM RSV-loaded liposomes seem to protect cells against where exposed to H_2O_2.

4.4 RSV loaded liposomes enhance mitochondrial fragmentation and vacuolar internalization

Autophagy protects organelles, cells, and organisms against several stress conditions. Although autophagy has widely been conceived as a self-destructive mechanism that causes cell death, accumulating evidence suggests that autophagy usually mediates cytoprotection, thereby avoiding the apoptotic or necrotic demise of stressed cells, and could mediate lifespan extension by RSV[64]. As reported elsewhere, sirtuin 1 was the first protein demonstrated to prolong lifespan in yeast (and then in animals including *Caenorhabditis elegans* and flies)[33, 65]and has also been shown to trigger autophagy in human and murine cultured cells[64]. Interestingly, RSV induces autophagy in yeast, which was shown to require the nicotinamide adenine dinucleotide–dependent deacetylase sirtuin 1 (SIRT1)[33,66,65]. In accordance, we found that after 45 h of incubation, both free and encapsulated RSV (100-200 µM) induce mitochondrial fragmentation and increase the number of yeast cells with mitochondrial vacuolar internalization, though more prominently with the loaded formulations. This same trend was observed when yeast cells incubated with empty DODAB:MO liposomes were compared with control cells. The effect of loaded RSV seems therefore to reflect the sum of the effect of free RSV and of empty DODAB:MO liposomes and suggest an enhancement of autophagy through a ROS independent mechanism. Indeed, though a previous study supports a role of mitochondrial oxidation events in the activation of autophagy, the DHE staining assays performed with both free and encapsulated RSV demonstrate an anti-oxidant activity.

5. Conclusions

RSV loaded DODAB:MO (1:2) liposomal system reveals characteristics suitable for possible drug administration, since the particles are stable and homogeneous, have dimensions below 200 nm, and a large positive surface charge, thus preventing liposome aggregation and a good EE% and RL%. The partition coefficient of RSV in the lipid system indicates that it has a preferential partition for the lipid matrix rather than remaining in the aqueous medium. In addition, RSV is located at the DODAB polar head levels, which decreases the microviscosity of the system. This may have an impact on the antioxidant effect of RSV, since the predisposed location of the RSV surface will make its hydroxyl groups accessible to eliminate free radicals. The developed lipid formulation also exhibits a controlled release of RSV for approximately 50 h, which demonstrates a great improvement over the pharmacokinetics.

RSV loaded liposomes are successfully internalized by yeast cells most likely by endocytosis. RSV does not affect yeast growth and cell viability in the concentration range tested but protected the cell against oxidative stress much likely through the enhancement of and perturbed autophagy.

6. Future perspectives

Ongoing studies in our lab include a deeper evaluation of the mechanisms involved in the internalization of the RSV-loaded liposomes by yeast cells. In this regard, yeast mutants defective in endocytosis will be tested, and the effect of endocytic inhibitors, like wortmannin, evaluated. Moreover, other markers of autophagy such as cleavage of ATG8-GFP or the assessment of alkaline phosphatase activity will be monitored to further confirm the involvement of resveratrol on the activation of autophagy.

7. References

1. Tsao R.; Chemistry and biochemistry of dietary polyphenols. Nutrients, 2, 1231- 1246 (2010).

2. Ding Y., Yau H., Yao Y., Fai L.Y. & Zhang Z.; Protection of dietary polyphenols against oral cancer. Nutrients, 5, 2173 - 2191 (2013).

3. Signorelli P. & Ghidoni R.; Resveratrol as an anticancer nutrient: molecular basis, open questions and promises. Journal of Nutritional Biochemistry, 16, 449 - 466 (2005).

4. Khoddami A., Wilkes M., & Roberts T.H.; Techniques for analysis of plant phenolic compounds. Molecules, 18, 2328 - 2375 (2013).

5. Lu Z., Zhang Y., Liu H., Yuan J., Zeng Z. & Zou G.; Transport of a cancer chemopreventive polyphenol, resveratrol: interaction with serum albumin and haemoglobin. Journal of Fluorescence, 17, 580 - 587 (2007).

6. Moran W.B., Anderson F.P., Devery A., Cloonan S., Butler W. E., Varughese S., Draper, S. M. & Kenny P.T.M.; Synthesis, structural characterisation and biological evaluation of fluorinated analogues of resveratrol Brian. Bioorganic and Medicinal Chemistry, 17, 4510 - 4522 (2009).

7. Timmers S., Auwerx J. & Schrauwen P.; The journey of resveratrol from yeast to human. Aging, 4, 146 - 158 (2012).

8. Zunino S. J. & Storm D.H.; Resveratrol-induced apoptosis in acute lymphoblastic leukemia cells by modulation of the mitochondrial permeability transition pore. Cancer Letters, 240, 123 - 134 (2006)

9. Garcia-Garcia J., Micol V., Godos A. & Gómes-Fernandez J.; The cancer chemopreventive is incorporated into model membranes and inhibits protein kinase C α Activity. Archives of Biochemistry and Biophysics, 372, 382 - 388 (1999).

10. Galfi P., Jakusb J., Molnara T., Neogradya S. & Csordas A.; Divergent effects of resveratrol, a polyphenolic phytostilbene, on free radical levels and type of cell death induced by the deacetylase inhibitors butyrate and trichostatin A. Journal of Steroid Biochemistry & Molecular Biology, 94, 39 - 47 (2005).

11. Losa G.A.; Resveratrol modulates apoptosis and oxidation in human blood mononuclear cells. European Journal of Clinical Investigation, 33, 818 - 823 (2003).

12. Brisdelli F., D'Andrea G. & Bozzi A.; Resveratrol: A natural polyphenol with multiple chemopreventive properties. Current Drug Metabolism, 10, 530 - 546 (2009).

13. Luther D. J., Ohanyan V., Shamhart P. E., Hodnichak M. C., Sisakian H., Booth T. D., Meszaros G. & Bishayee A.; Chemopreventive doses of resveratrol do not produce cardiotoxicity in a rodent model of hepatocellular carcinoma. Invest New Drug, 29, 380 - 391 (2011).

14. Roy P., Kalra N., Prasad S., George J. & Shukla Y.; Chemopreventive potential in mouse skin tumors through regulation of mitochondrial and PI3K/AKT singnaling pathways. Pharmaceutical Research, 26, 211 - 217 (2009).

15. Neves A.R., Lúcio M., Lima J.L.C. & Reis S.; Resveratrol in medicinal chemistry: Acritical review of its pharmaokinetics, drug-delivery, and membrane interactions. Current Medicinal Chemistry, 19, 1663 - 1681 (2012).

16. Shi G., Rao L., Yu H., Xiang H., Yang, H. & Ji R.; Stabilization and encapsulation of photosensitive resveratrol within yeast cell. International Journal of Pharmaceutical, 349, 83 - 93 (2008).

17. Magalhães L.M., Nunes C., Lúcio M., Segundo M. A., Reis S. & Lima J.L.F.C.; High-throughput microplate assay for the determination of drug partition coefficients. Nature Protocols, 5, 1823 - 1830 (2010).

18. Neves A.R., Lúcio M., Martins S., Lima J.L.F.C. & Reis S.; Novel resveratrol nanodelivery systems based on lipid nanoparticles to enhance its oral bioavailability. International Journal of Nanomedicine, 8, 177 - 187 (2013).

19. Bamrungsap S., Zhao Z., Chen T., Wang L., Li C., Fu T. & Tan W.; Nanotechnology in therapeutics: a focus on nanoparticles as a drug delivery system. Nanomedicine, 7, 1253 - 1271 (2012).

20. Deshpande P.P., Biswas S. & Torchilin V.; Current trends in the use of liposomes for tumor targeting. Nanomedicine, 8, 1509 - 1528 (2013).

21. Lindman P. & Alexandridis P.; Amphiphilic molecules: small and large. Amphiphilic block copolym, Physical Chemistry 1, Center for Chemistry and Cemical Engeineering, and Center for Amphiphilic Polymers from Renewable Resources, Ludon iniversity, P.O. Box 124, Lund S-22100, Sweden, 1 - 12 (2000).

22. Jesorka A. & Orwar O.; Liposomes: Technologies and analytical applications. Annual Review of Analytical Chemistry, 1, 801 - 832 (2008).

23. Elizondo E., Moreno E., Cabrera I., Córdoba A., Sala S., Veciana J., Ventosa N.; Liposomes and other vesicular systems: structural characteristics, methods of preparation, and use in nanomedicine. In Progress in Molecular Biology and Translational Science, 104, 1 - 52, (2011).

24. Silva J.P.N., Oliveira A.C.N., Casal M.P.P.A., Gomes A.C., Coutinho P.J.G., Coutinho O.P., Real Oliveira M.E.C.D.; DODAB:monoolein-based lipoplexes as non-viral vector for transfection of mammalian cells. Biochimica et Biophysica Acta, 1808, 2440 - 2449 (2011).

25. Oliveira I.M.C.S., Silva J.P.N., Feitosa E., Marques E.F., Castanheira E.M.S., Real Oliveira M.E.C.D.; Aggregation behavior of aqueous dioctadecyldimethylammonium bromide/monoolein mixtures: A multitechnique investigation on the influence of composition and temperature. Journal of Colloid and Interface Science, 374, 206 - 217 (2012).

26. Silva J.P.N., Oliveira A.C.N., Gomes A.C. & Real Oliveira M.E.C.D.; Development of Dioctadecyldimethylammoniumbromide/monoolein liposomes for gene delivery *in* Cell Interaction, Gowder S. ed., Intech (2012).

27. Silva J.P. N., Oliveira I.M.S.C, Oliveira A.C.N., Lúcio M., Gomes A.C., Coutinho P.J.G., Real Oliveira M.E.C.D.; Structural dynamics and physicochemical properties of pDNA/DODAB: MO lipoplexes: Effect of pH and anionic lipids in inverted non-lamellar phases versus lamellar phases. Biochim et Biophys Acta, 1838, 2555 - 2567 (2014).

28. Oliveira A.C.N, Martens T.F., Raemdonck K., Adati R.D., Feitosa E., Botelho C., Gomes A.C., Braeckmans K. & Real Oliveira M.E.C.D.; Dioctadecyldimethylammonium: Monoolein nanocarriers for efficient *in vitro* gene silencing. American Chemical Society Applied Materials & Interfaces, 6, 6977 - 6989 (2014).

29. Ferreira, I.S.; Lipid based nanocarriers for the delivery of the bioactive compound resveratrol, Tese de Mestrado em Biofísica e Bionanossistemas. Repositório Universidade do Minho , 1 - 119 (2015).

30. Porcu M. & Chiarugi A.; The emerging therapeutic potential of sirtuin-interacting drugs: from cell death to lifespan extension. Trends in Pharmacological Sciences, 26, 94 - 103 (2005).

31. Xie Z. & Klionsky D.J.; Autophagosome formation: core machinery and adaptations. Nature Cell Biology, 9, 1102 - 1109 (2007).

32. Gershon H. & Gershon D.; The budding yeast, *Saccharomyces cerevisiae*, as a model for aging research: a critical review. Mechanisms of Ageing and Development, 120, 1 - 22 (2000).

33. Howitz K.T., Bitterman K.J., Cohen H.Y., Lamming D.W., Lavu S., Wood J.G., Zipkin R.E., Chung P., Kisielewski A., Zhang L., Scherer B. & Sinclair D.A.; Small molecule activators of sirtuins extend *Saccharomyces cerevisiae* lifespan. Nature, 425, 191 - 196 (2003).

34. Wang X., Wang D. & Zhao Y.; Effect and mechanism of resveratrol on the apoptosis of lung adenocarcinoma cell line A549. Cell Biochemistry Biophysics, 73, 527 – 531 (2015).

35. Weissig V.; liposomes-methods and protocolsIs. Pharmaceutical Nanocarriers, 606, 21-30 (2010).

36. Veal E.A., Ross S.J., Malakasi P., Peacock E. & Morgan B.A; Ybp1 is required for the hydrogen peroxide-induced oxidation of the Yap1 transcription factor. The Journal of Biological Chemistry, 278, 30896 – 30904 (2003).

37. Fini L., Hotchkiss E., Fogliano V., Graziani G., Romano M., Edward B., Qin H., Selgrad M., Boland C.R., & Ricciardiello L.; Chemopreventive properties of pinoresinol-rich olive oil involve a selective activation of the ATM-p53 cascade in colon cancer cell lines. Carcinogenesis, 29, 139 - 46 (2008).

38. Erk V.M.J., Roepman P., Lende T.R.V., Stierum R.H., Aarts J.M.M.J.G., Bçaderen P.J.V. & Ommen B.V.; Integrated assessment by multiple gene expression analysis of quercetin bioactivity on anticancer-related mechanisms in colon cancer cells in vitro. European Journal of Nutrition, 44, 143 - 56 (2005).

39. Breeuwer P., Drocourt J.L., Bunschoten N., Zwietering M.H., Rombouts F.M. & Abee T.; Characterization of uptake and hydrolysis of fluorescein diacetate and carboxyfluorescein diacetate by intracellular esterases in *Saccharomyces cerevisiae*, which result in accumulation of fluorescent product. Applied and Environmental Microbiology, 61, 1614-1619 (1995).

40. Kalyanaramana B., Darley-Usmarb V., Daviesc K.J.A., Dennerye P.A., Formanc H.J.F, Grishamg M.B., Mannh G.E., Moorei K., Roberts L.J. & Ischiropoulose H.; Measuring reactive oxygen and nitrogen species with fluorescent probes: challenges and limitations balaraman. Journal of Health Institutes, 52, 1 - 6 (2011).

41. Westerman B. & Neupert W.; Mitochondria-targeted green fluorescent proteins: convenient tools for the study of organelle biogenesis in *Saccharomyces cerevisiae*. Yeast Functional Analysis Report, 16, 1421 - 1427 (2000).

42. Carneiro C., Correia A., Collins T., Vilanova M., Pais C., Gomes A.C., Real Oliveira M.E.C.D. & Sampaio P.; DODAB:monoolein liposomes containing Candida albicans cell wall surface proteins: A novel adjuvant and delivery system. European Journal of Pharmaceutics and Biopharmaceutics, 89, 190 - 200 (2015).

43. Carneiro C., Correia A., Lima T., Vilanova M., Pais C., Gomes A.C., Real Oliveira M.E.C.D. & Sampaio P.; Protective effect of antigen delivery using monoolein-based liposomes in

experimental hematogenously disseminated candidiasis. Acta Biomaterialia, 39, 133 - 145 (2016).

44. Csiszár A., Pinto J.T., Gautam T., Kleusch C., Hoffmann B., Tucsek Z., Toth P., Sonntag W.E. & Ungvari Z.; Resveratrol encapsulated in novel fusogenic liposomes activates Nrf2 and attenuates oxidative stress in cerebromicrovascular endothelial cells from aged rats. Journals of Gerontology Series A: Biological Sciences and Medical, 70, 303 - 313 (2015).

45. Kobayashi H., Watanabe R. & Choyke P.L.; Review Improving conventional enhanced permeability as retention (EPR) effects; What is the appropriate target? Theranostics, 4, 81–89 (2014).

46. Engelke M., Bojarski P., Bloß R. & Diehl H.; Tamoxifen perturbs lipid bilayer order and permeability: comparison of DSC, fluorescence anisotropy, laurdan generalized polarization and carboxyfluorescein leakage studies. Biophysical Chemistry, 90, 157 - 173 (2001).

47. Brittes J., Lúcio M., Nunes C., Lima J.L.F.C. & Reis S.; Effects of resveratrol on membrane biophysical properties: relevance for its pharmacological effects. Chemistry and Physics of Lipids, 163, 747 - 754 (2010).

48. Sprouse A.A. & Herbert, B.; Resveratrol augments paclitaxel treatment in MDA-MB-231and paclitaxel resistant MDA-MB-231 breast cancer cells. Anticancer Reseach, 34, 5363 - 5374 (2014).

49. Schuster S., Penke M., Gorski T., Petzold-Quinque S., Damm G., Gebhardt R., Kiess W., & Gerten A.; Resveratrol differentially regulates NAMPT and SIRT1 in hepatocarcinoma cells and primary human hepatocytes. PLoS One, 9, 1 - 15 (2014).

50. Vanamala J., Reddivari L., Radhakrishnan S. & Tarver C.; Resveratrol suppresses IGF-1 induced human colon cancer cell proliferation and elevates apoptosis via suppression of IGF-1R/Wnt and activation of p53 signaling pathways. Biomed Central Cancer, 10, 1 - 14 (2010).

51. Taylor E.J.M., Yu Y., Champer J. & Kim J.; Resveratrol demonstrates antimicrobial effects against propionibacterium acnes in vitro. Dermatol Ther, 4, 249 – 257 (2014).

52. Wang Z., Gu Z., Shen Y., Wang Y., Li J., Lv H., & Huo K.; The natural product resveratrol inhibits yeast cell separation by extensively modulating the transcriptional landscape and reprogramming the intracellular metabolome. PLoS ONE, 1 - 20 (2016).

53. Madrigal-Perez L.A., Canizal-Garcia M., González-Hernández J.C., Reynoso-Camacho R., Nava G.M. & Ramos-Gomez M.; Energy-dependent effects of resveratrol in *Saccharomyces cerevisiae*. Yeast, 33, 227 - 234 (2016).

54. Madrigal-Perez L.A., Nava G.M., González-Hernández J.C. & Ramos-Gomez M.; Resveratrol increases glycolytic flux in *Saccharomyces cerevisiae* via a SNF1-dependet mechanism. J Bioenerg Biomembr, 47, 331 - 336 (2015).

55. Nagataand T. & Toe A. Japan Patent 107183 (1983).

56. Bishop J.R.P., Nelson G. & Lamb J.; Microencapsulation in yeast cells. Journal of Microencapsulation, 15, 761- 773 (1998).

57. Escoté X., Miranda M., Menoyo S., Rodríguez-Porrata B., Carmona-Gutiérrez D., Jungwirth H., Madeo F., Cordero R.R., Mas A., Tinahones F., Clotet J. & Vendrell J.; Resveratrol induces antioxidant defence via transcription factor Yap1p. Yeast, 29, 251 - 263 (2012).

58. Martins L.A.M., Coelho B.P., Behr G., Pettenuzzo L.F., Sousa I.C.C., Moreira J.C.F., Borojevic R., Gottfriend C. & Guma F.C.R.; Resveratrol Induces Pro-oxidant Effects and Time-Dependent Resistance to Cytotoxicity in Activated Hepatic Stellate Cells. Cell Biochem Biophys, 68, 247 - 25 (2014).

59. Lastra C.A. & Villegas I.; Resveratrol as an antioxidant and pro-oxidant agent: mechanisms and clinical implications. Biochemical Society Transactions, 35, 1156 - 1160 (2007).

60. Quicozes-Santos A., Andreazza A. C., Gonçalves C. A., & Gottfried, C.; Actions of redox-active compound resveratrol under hydrogen peroxide insult in C6 astroglial cells. Toxicology in Vitro, 24, 916 - 920 (2010).

61. Joe A. K., Liu H., Suzui M., Vural M. E. Xiao D., & Weinstein I. B.; Resveratrol induces growth inhibition, S-phase arrest, apoptosis, and changes in biomarker expression in several human cancer cell lines. Clinical Cancer Research, 8, 893 - 903 (2002).

62. Souza I. C., Martins L. A., Coelho B. P., Grivicich I., Guaragna R. M. & Gottfried C.; Resveratrol inhibits cell growth by inducing cell cycle arrest in activated hepatic stellate cells. Molecular and Cellular Biochemistry, 315, 1–7 (2008).

63. Juan M. E., Wenzel U., Daniel H., & Planas J. M.; Resveratrol induces apoptosis through ROS-dependent mitochondria pathway in HT-29 human colorectal carcinoma cells. Journal of Agriculture and Food Chemistry, 56, 4813–4818 (2008).

64. Morselli E., Galluzzi L., Kepp O., Criollo A., Maiuri M.C., Tavernarakis N., Madeo F., & Kroemer G.; Autophagy mediates pharmacological lifespan extension by spermidine and resveratrol. Aging, 1, 961-970 (2009).

65. Finkel T., Deng C.X. & Mostoslavsky R.; Recent progress in the biology and physiology of sirtuins. Nature, 460, 587 - 591 (2009).

66. Lee I.H., Cao L., Mostoslavsky R., Lombard D.B., Liu J., Bruns N.E., Tsokos M., Alt F.W. & Finkel T.; A role for the NAD-dependent deacetylase Sirt1 in the regulation of autophagy.

Proceeding of the National Academy of Sciences of United States of America, 105, 3374

- 3379 (2008).